The F2-Isoprostane:Thromboxane-prostanoid receptor signaling axis drives persistent fibroblast activation in pulmonary fibrosis

Toshio Suzuki
Vanderbilt University Medical Center https://orcid.org/0000-0002-0909-0466
Jonathan Kropski
Vanderbilt University Medical Center
Jingyuan Chen
Vanderbilt University Medical Center
Erica Carrier
Vanderbilt University Medical Center
Xinping Chen
Vanderbilt University Medical Center
Taylor Sherrill
Vanderbilt University Medical Center
Vasily Polosukhin
Vanderbilt University Medical Center
Wei Han
Vanderbilt University Medical Center
Anandharajan Rathinasabapathy
Vanderbilt University Medical Center https://orcid.org/0000-0002-3474-8063
Sergey Gutor
Vanderbilt University Medical Center
Peter Gulleman
Vanderbilt University Medical Center
Nicholas Banovich
The Translational Genomics Research Institute
Harikrishna Tanjore
Vanderbilt University Medical Center
Michael Freeman
Vanderbilt University Medical Center
Yuji Tada
International University of Health and Welfare
Lisa Young

Vanderbilt University Medical Center
Jason Gokey
Vanderbilt University Medical Center
Timothy Blackwell
Vanderbilt University Medical Center
James West (j.west@vumc.org)
Vanderbilt University Medical Center

Article

Keywords: pulmonary fibrosis, Idiopathic Pulmonary Fibrosis (IPF), F2-Isoprostane

Posted Date: January 13th, 2021

DOI: https://doi.org/10.21203/rs.3.rs-141939/v1

Abstract

While transient fibroblast activation is a normal and adaptive aspect of injury-repair in many contexts, persistent fibroblast activation is a hallmark of idiopathic pulmonary fibrosis (IPF) and other chronic fibrotic lung diseases. The mechanisms regulating persistent fibroblast activation in IPF have not been fully elucidated. In the lungs of IPF patients and in mice with experimental lung fibrosis, we observed that expression of the thromboxane-prostanoid receptor (TBXA2R) was increased in fibroblasts. Genetic deletion of TBXA2R, but not inhibition of thromboxane synthase, protected mice from bleomycin-induced lung fibrosis, suggesting an alternative ligand activates profibrotic TBXA2R signaling. We found that F2-isoprostanes (F2-IsoPs), nonezymatic products of arachidonic acid metabolism generated in the setting of reactive oxygen species (ROS), are persistently elevated in experimental lung fibrosis and act as an alternative TBXA2R ligand. Further studies demonstrated that F2-isoprostanes signal through TBXA2R to activate Smad signaling, revealing TBXA2R as a previously unrecognized regulator of the transforming growth factor beta (TGF-β) pathway. Further, treatment with the small-molecule TBXA2R antagonist ifetroban protected mice from lung fibrosis in three pre-clinical models: bleomycin treatment, Hermansky-Pudlak Syndrome, and radiation-induced fibrosis. Importantly, treatment with ifetroban during the fibrotic phase of bleomycin injury markedly enhanced fibrotic resolution. Together, these studies implicate TBXA2R signaling as a crucial mediator linking oxidative stress to fibroblast activation and indicate that TBXA2R antagonists could be efficacious for treatment of IPF and other chronic fibrotic disorders.

Introduction

Idiopathic Pulmonary Fibrosis (IPF) is a chronic, progressive syndrome that is characterized by destruction of the gas-exchange units of the lung and pathologic accumulation of extracellular matrix (ECM).[1,2] Despite decades of work, the underlying mechanisms driving progressive pulmonary fibrosis remain incompletely understood, and most patients with IPF succumb to their disease within 3-5 years of diagnosis.[1] Injury to and dysfunction of the lung epithelium is hypothesized to play a prominent role in disease initiation,[3,4] while fibroblasts are the primary effector cell type producing pathologic ECM[5,6] and are the target of FDA-approved IPF therapies.[7,8] The mechanisms underlying persistent fibroblast activation in IPF remain incompletely understood.

Oxidative stress and elevated production of reactive oxygen species (ROS) have been implicated as key features of the dysfunctional lung/alveolar epithelium in IPF,[9,10] and have been associated with fibroblast activation.[11] Our group previously demonstrated that there is extensive accumulation of isolevaglandin-adducted proteins in IPF lung tissue,[12] suggesting ROS generation is widespread and persistent in the fibrotic lung. In the setting of elevated ROS, arachidonic acid metabolites undergo nonenzymatic conversion to a series of compounds known as F2-isoprostanes (F2-IsoPs).[13] F2-IsoPs have been widely used as a biomarker of oxidative stress, prior studies have demonstrated the F2-IsoP's may also play direct signaling roles, including activation of hepatic stellate cells through the thromboxane-prostanoid receptor (TBXA2R).[14–16]

In these studies, we determined that TBXA2R expression is increased during lung fibrosis, particularly in fibroblasts, where ligand binding by F2-IsoPs mediates fibroblast activation. Together, these investigations define a novel mechanism by which ROS contribute to fibrogenesis and implicate TBXA2R as a regulator of transforming-growth-factor beta (TGF-β) signaling. Our findings highlight TBXA2R as a promising new therapeutic target for treatment of pulmonary fibrosis.

Results

TBXA2R expression in fibroblasts is increased during lung fibrosis in mice and humans

To determine the role of TBXA2R in pulmonary fibrosis, we first investigated TBXA2R expression in the lungs of IPF patients. In lung tissue lysates, quantification of TBXA2R by western blot demonstrated significantly higher TBXA2R levels in IPF compared to control lungs **(Fig. 1a)**. Examining single-cell RNA sequencing (scRNA-seq) data generated from pulmonary fibrosis and non-fibrotic control (declined donor) lungs that our group has recently reported,[6] we observed that *TBXA2R* expression was detected in fibroblasts in addition, to endothelial cells and smooth muscle cells (**Fig. 1b**). Consistent with transcriptomic data, dual immunofluorescence staining showed TBXA2R co-localized with a fibroblast marker (S100A4) in areas of fibrotic remodeling in IPF lung tissue sections, but co-staining was not observed in lung parenchyma from nonfibrotic controls (**Fig. 1c**). In mouse lung tissue, TBXA2R expression increased following bleomycin challenge as measured by western blot (**Fig. 1d**), and similar to our observation in IPF lung tissue, TBXA2R expression was localized to areas of fibrosis and colocalized with the fibroblast marker S100A4 (**Fig. 1e**). Together, these data raised the possibility of a previously unrecognized role for TBXA2R signaling in regulating fibroblast activity during pulmonary fibrosis in mice and humans.

To test the effects on TBXA2R signaling on lung fibrosis, we generated inducible TBXA2R deficient mice by crossing TBXA2R-floxed mice (*TBXA2R*$^{f/f}$) with a universal tamoxifen inducible Cre-recombinase line (see Methods) (*TBXA2R*^{iKO} hereafter). These mice develop normally and have no spontaneous phenotype except for a mildly increased bleeding time.[17] Tamoxifen treatment (400 mg/kg chow ad libitum for 14 days) led to ~75% reduction in TBXA2R protein in lung tissue (**see Extended Data Fig. 1a,b**). The resulting *TBXA2R*^{iKO} and age-matched adult WT controls were treated with tamoxifen and then challenged with IT bleomycin (0.04 units). At day 21 post-bleomycin, *TBXA2R*^{iKO} mice had a striking reduction in lung fibrosis as determined by morphometric analysis (**Fig. 1f,g and see Extended Data Fig. 1c**) and measurement of hydroxyproline content (**Fig. 1h**). In contrast to genetic deletion of TBXA2R, treatment with ozagrel, a small-molecule inhibitor of the enzyme responsible for generation of TXA_2,[18] failed to protect mice from bleomycin-induced fibrosis (**Fig. 1i,j,k**), thereby indicating that an alternative ligand is responsible for profibrotic TBXA2R signaling.

F2-isoprostanes induce TBXA2R signaling in pulmonary fibrosis

F_2-isoprostanes (F_2-isoPs) are a non-enzymatic product of free radical-induced peroxidation of arachidonic acid[13] that are increased in the lungs of IPF patients,[19] as well as other conditions where reactive oxygen species (ROS) are produced.[13] F_2-isoPs have structural similarities to TXA_2 and can activate TBXA2R signaling.[16] We measured F2-IsoPs and thromboxane B2 (TxB2), the major stable metabolite of TxA2, in the lungs of mice at baseline and after IT bleomycin. TxB2 was increased in lung tissue by day 1 post-bleomycin and subsequently returned towards baseline by day 7 (**Fig. 2a**). In contrast, F2-IsoPs were increased in the lungs throughout the 21-day time course (**Fig. 2b**).

To determine whether F2-IsoPs are responsible for TBXA2R-driven pro-fibrotic phenotypes in lung fibroblasts, we isolated mouse-lung fibroblasts (MLFs) from WT and tamoxifen-treated *TBXA2R*^{iKO} mice and cultured these cells in serum-containing media, which contains isoprostanes[20]. When grown on tissue culture plates in serum-containing media, *TBXA2R*^{iKO} MLFs had ~50% reduced proliferation compared to WT MLFs (**Fig. 2c**). Under low serum conditions (2.5%), however, *TBXA2R*^{iKO} MLFs had similar BrdU incorporation compared to WT. In low serum conditions, addition of F2-IsoPs (100 nM, Cayman Chemicals) to the culture medium enhanced proliferation of WT but not TBXA2R deficient MLFs (**Fig. 2d**). In addition, treatment with F2-IsoPs induced α-SMA expression in WT MLFs but not *TBXA2R*^{iKO} MLFs (**Fig. 2e,f**). We also measured Collagen 1 expression by western blot (**Fig. 2g**) and collagen accumulation in media (**Fig. 2h**) and found that F2-IsoPs upregulated collagen synthesis and secretion by WT MLFs but not *TBXA2R*^{iKO} MLFs. Together, these studies indicated a specific role for F2-isoprostane-induced TBXA2R signaling in fibroblast activation.

TBXA2R regulates TGF-β signaling

The observation that F2-isoprostane signaling through TBXA2R led to fibroblast activation resembled responses classically induced by transforming-growth-factor beta (TGF-β), and suggested a potential interaction with TGF-β signaling. To determine whether there is a direct interaction between TBXA2R and TGF-β signaling, we transfected WT and *TBXA2R*^{iKO} MLFs with a reporter of TGF-β activation, a Smad2/3 binding element (SBE)-driven luciferase construct. Forty-eight hours after transfection, addition of F2-IsoPs increased luciferase activity (**Fig. 3a**) and induced canonical and non-canonical TGF-β pathway activation in WT MLFs but not *TBXA2R*^{iKO} MLFs (**Fig. 3b-c**). Stimulation of fibroblasts with a specific TBXA2R agonist U-46619 (100 nM, Cayman Chemicals) showed similar effects to treatment with F2-IsoPs (**see Extended Data Fig. 2**). In contrast, *ex-vivo* deletion of TBXA2R from MLF isolated from bleomycin-challenged mice resulted in a marked decrease in fibrosis-related protein expression, including Collagen type I, Timp1, Smad2/3 phosphorylation, Akt-phosphorylation and p44/42-phosphorylation (**Fig. 3d**) as well as *Acta2*, *Col1a1*, *Col1a2* and *SerpinE1* gene expression levels (**Fig. 3e**). Together these studies demonstrated that F2-IsoPs promote fibroblast activation and proliferation through TBXA2R-mediated potentiation of TGF-β signaling.

TBXA2R-induced calpain activity mediates downstream activation of TGF-β

We next sought to determine the mechanisms connecting TBXA2R signaling to TGF-β activation. First, we treated *TBXA2R*^{iKO} and control MLFs with recombinant human TGF-β1 (10 nM, R&D Systems) and evaluated SBE luciferase reporter activity at 4 hours. TGF-β1-induced Smad activation was not attenuated in *TBXA2R*^{iKO} MLFs (**Fig. 4a**). Similarly, there was no attenuation of TGF-β1-induced gel contraction in *TBXA2R*^{iKO}MLFs (**Fig. 4b**). These results showed that TBXA2R is not required for TGF-β pathway activation when active TGF-β is added directly to cells. We next tested whether TBXA2R-dependent activation of the TGF-β pathway by F2-IsoPs requires TGF-β receptors. Treatment of MLFs with F2-IsoPs induced robust induction of TGF-β targets *SerpinE1* and *Timp1*, which was prevented by addition of the TGF-β receptor inhibitor LY2109761 (**Fig. 4c**). These findings suggested that TBXA2R signaling does not activate TGF-β signaling independent of the TGF-β receptor complex.

In fibroblast cultures, TGF-β is primarily bound by a latent TGF-β binding protein (LTBP), either as part of a latent extracellular pool, or, in some cell types, intracellularly[21]. In this context, the calcium-dependent cysteine protease calpain-4 has been shown to activate TGF-β and induce Smad2/3 phosphorylation, likely by activating TGF-β in endosomal vesicles[21]. In light of the well-established effects of TBXA2R signaling on calcium flux[22], we investigated whether F2-IsoPs could induce calpain activation in fibroblasts. Treatment of primary lung fibroblasts from WT mice with F2-IsoPs (100 nM) significantly increased calpain activity (**Fig. 4d**). Subsequent studies showed that addition of a calpain inhibitor (Z-LLY-FMK, 30 μM) blocked F2-IsoP induction of Smad2/3 signaling, collagen type I protein expression, and *Serpine1*/ *Timp2* gene expression (**Fig. 4e-g**). Cumulatively, these studies support the conclusion that F2-IsoP induction of TBXA2R signaling stimulates calpain-induced activation of latent TGF-β, thus leading to downstream activation of the TGF-β pathway.

Ifetroban attenuates profibrotic TBXA2R signaling in fibroblasts

Having established that F2-IsoP signaling through TBXA2R potentiates the TGF-β pathway, we hypothesized that antagonizing TBXA2R could inhibit fibroblast activation. To test this, we isolated MLF from WT mice and stimulated them with F2-IsoPs in the presence of a small molecule TBXA2R antagonist (Ifetroban, 0.3 μM) or vehicle. Ifetroban (originally known as BMS-180,291), is a highly selective, potent (IC50 ~1020 nM), orally available TBXA2R antagonist.[23] Ifetroban treatment reduced Smad2/3, p44/42, and Akt phosphorylation, as well as Timp1 and α-sma protein levels (**Fig. 5a**), indicating that Ifetroban inhibits F2-IsoP-driven fibroblast activation in MLFs.

We then examined whether TBXA2R antagonism could similarly prevent activation of human lung fibroblasts. We isolated fibroblasts from explanted lungs of IPF patients and treated these cells *ex vivo* with Ifetroban (0.3 μM). In these studies, Ifetroban treatment significantly inhibited migration (scratch wound closure) (**Fig. 5b**), proliferation (**Fig. 5c**), pro-fibrotic signaling pathway activation, and expression of pro-fibrotic genes, including α-smooth muscle actin (*α-SMA*), collagen type 1, and serpin E1 (**Fig. 5d,e**), further supporting the conclusion that signaling through TBXA2R regulates important pro-fibrotic functions of lung fibroblasts.

Ifetroban treatment attenuates fibrosis in mouse models of lung fibrosis.

To test whether pharmacological inhibition of TBXA2R could be used therapeutically to prevent or treat lung fibrosis, we treated wild-type (WT) mice (C57Bl/6 background) with Ifetroban (25 mg/kg/day in drinking water) or standard drinking water (vehicle) beginning 3 days before a single intratracheal (IT) injection of bleomycin (0.04U) or beginning on day 7 post-bleomycin and continuing until harvest at day 21. As shown in **Figure 6**, Ifetroban treatment blocked bleomycin-induced fibrosis when administered for the entire 21-day course or administered only during the fibrotic phase (day 7-21), as assessed by morphometric analysis (**Fig. 6a,b**) and hydroxyproline content (a major component of collagen) (**Fig. 6c**). While epithelial apoptosis and inflammation, have been correlated with subsequent fibrosis [24–27] in the bleomycin model, Ifetroban did not affect epithelial apoptosis (**Extended Data 3a-b**) or inflammatory cell recruitment (**Extended Data Fig. 4**). To determine whether Ifetroban treatment could hasten resolution of fibrosis, we performed additional experiments where drug or vehicle was started on day 14 and continued until day 28 (**Fig. 6d**). In these studies, Ifetroban attenuated weight loss (**Fig. 6e**) and accelerated resolution of fibrosis (**Fig. 6f-h**). Cumulatively, studies in the bleomycin model showed that Ifetroban reduces fibrosis and enhances resolution when given during the fibrotic phase of bleomycin-induced fibrosis without affecting bleomycin-induced inflammation or epithelial apoptosis, thereby suggesting direct effects of TBXA2R signaling on fibrogenesis. Proteins associated with fibrosis, including Tissue Inhibitor of Metalloproteinase-1 (Timp-1) and Smad2 phosphorylation downstream of canonical TGF-β signaling, were both strongly induced by bleomycin and blocked by Ifetroban treatment (**Fig. 6i-k**).

We next tested whether Ifetroban could prevent fibrosis in a model of genetic susceptibility to lung fibrosis, Hermansky-Pudlak Syndrome (HPS). HPS is an autosomal recessive disease in which several of the genetic subtypes (HPS1, HPS2, and HPS4) have highly penetrant pulmonary fibrosis with onset in early adulthood.[28] Naturally occurring mutations in HPS mice reliably model important features of the human disease, including susceptibility to pro-fibrotic stimuli.[29–31] To induce fibrosis in HPS mice, low doses of bleomycin (0.025 units) delivered by IT injection result in a rapidly progressive pulmonary fibrosis phenotype.[29–31] We treated HPS1 mice and HPS2 mice (with loss-of-function mutations in the HPS1 gene or the HPS2 gene, respectively) with Ifetroban beginning on the day prior to IT bleomycin and continuing until day 7 post-bleomycin, when lungs were harvested. Ifetroban treatment significantly attenuated lung fibrosis in HPS1 (**Fig. 7a**) and HPS2 mice (**Fig. 7b,c**) as determined by measurement of lung collagen.

We also used a model of radiation-induced fibrosis to investigate the anti-fibrotic effects of Ifetroban. Immediately following thoracic irradiation (17 Gy), mice were administered Ifetroban in drinking water or vehicle and continued treatment until lungs were harvested 4 months post-irradiation. Compared to placebo, Ifetroban-treated mice had significantly reduced lung collagen content following exposure to ionizing radiation (**Fig. 7d,e**). Together, these data indicate that TBXA2R is a promising therapeutic target for lung fibrosis.

Discussion

Transient fibroblast activation is an adaptive process that is crucial for wound and other forms of injury-repair. While there has been considerable progress made in understanding the signaling and molecular processes that activate fibroblasts in the lung and other organs during injury-repair, the mechanisms that lead to persistent and pathologic fibroblast activation remain less well-defined. In these studies, we demonstrate a novel paradigm linking oxidative stress to persistent fibroblast activation through F2-IsoP-induced TBXA2R signaling, which is a previously unrecognized regulator of the TGF-β pathway.

In the context of lung fibrosis, ROS are produced by a variety of cells, including epithelial cells[10,32] and fibroblasts.[33,34] NADPH oxidase 4 has been shown to be an important source of ROS in lung fibrosis.[11,35] ROS have been shown to enhance fibroblast proliferation, induce collagen formation,[34] and promote apoptosis-resistance.[35–37] F2-IsoPs are produced by non-enzymatic conversion of arachidonic acid in the presence of ROS[13,19] and have been shown to function as an alternative ligand for TBXA2R.[38,39] F2-IsoPs are increased in serum, BAL, and exhaled breath condensate from IPF patients[40–42] and have previously been suggested to contribute to bleomycin-induced fibrosis in rats.[43] Our findings indicate that F2-IsoPs can mediate the effects of ROS on fibroblasts and that F2-IsoP-induced fibroblast activation can be prevented by TBXA2R antagonism or genetic deletion.

Although TBXA2R performs diverse functions beyond platelet biology, its role in lung fibrosis has not been previously investigated. Mechanistically, we found TBXA2R signaling in fibroblasts induces TGF-β signaling through a calpain-dependent mechanism. TGF-β is a master regulator of mesenchymal responses in physiological and pathological conditions, and persistent activation of TGF-β signaling has been described as a hallmark of pulmonary fibrosis. While mechanical forces[44] and other factors likely play a role in fibroblast activation during pulmonary fibrosis,[45–47] the molecular mechanisms that underlie the persistence of TGF-β activity in this setting remain uncertain. It has previously been recognized that oxidative stress can be associated with activation of latent TGF-β activation,[48,49] but the specific mechanisms have not been determined. After translation, TGF-β is bound by LTBPs to maintain an inactive state. TGF-β can be activated or released from LTBPs through a variety of mechanisms,[50] including cleavage of LTBPs by the calcium-dependent cysteine protease calpain-4,[21] and downstream signaling through the TGF-β pathway interacts with numerous other pathways that mediate and modulate the biological effects of TGF-β.[51] Our data extend knowledge in this area by showing that TBXA2R signaling induces calpain activity in fibroblasts, which in turn mediates down-stream TGF-β activation. Consistent with this paradigm, calpain inhibition in fibroblasts reduced F2-IsoP-induced Smad2/3 signaling and inhibited profibrotic gene expression.

While these data provide compelling evidence that TBXA2R signaling is involved in pulmonary fibrosis, there are important limitations of these studies. First, there are likely cell-type specific effects of TBXA2R in endothelial cells, smooth muscle cells, and platelets that may also impact fibrogenesis in the lungs. Further studies will be required to discern the effects of TBXA2R antagonism in these cell types on

fibrogenesis. Second, we have not conclusively shown that F2-IsoPs are the major ligand for activation of TBXA2R signaling during *in-vivo* lung fibrosis. This would require a strategy to reduce ROS, which would likely have additional effects on lung fibrosis not mediated directly through TBXA2R. Third, additional work is required to determine whether TBXA2R is an important therapeutic target in fibrotic lung diseases other than IPF and fibrotic conditions in other organs.

Together, these studies have demonstrated a key role of TBXA2R-signaling in pulmonary fibrosis, and TBXA2R represents an attractive target with translational potential. In these experiments, we demonstrate the small-molecule ifetroban effectively inhibits TBXA2R signaling and pulmonary fibrosis in multiple experimental models. Ifetroban and other TBXA2R antagonists have been or are currently in human studies for secondary prevention of coronary artery disease,[52] allergic asthma,[53] and other conditions,[54–57] and appear to be safe and well-tolerated.

In summary, we have implicated TBXA2R-signaling as a key pathway in pulmonary fibrosis. These studies offer the potential for rapid translation into clinical trials with the goal of improving outcomes in IPF.

Methods

Subjects and Samples

IPF tissue samples were obtained from explanted lungs removed at the time of lung transplantation. Nonfibrotic control tissue samples were obtained from lungs declined for organ donation.

Mouse Models

TBXA2R floxed mice[17] were obtained from Jackson Labs (#21985) . These mice have loxp sites surrounding *TBXA2R* exon 2, which under the influence of Cre recombinase is excised, eliminating protein production. They had been backcrossed onto a B6 strain. These were crossed to mice with tamoxifen-inducible cre expression under the control of the universally expressed Rosa26 locus (*Rosa26-CreER, Jackson Labs #4847*).[58] In combination, these *Rosa26-CreER*$^{+}$*TBXA2R*$^{f/f}$ mice are referred to as TBXA2R^{iKO}, and have global deletion of TBXA2R when induced by Tamoxifen. Hermansky-Pudlak Syndrome mice included “pale ear” mice (Jackson Laboratories #525) which carry a constitutive mutation in *Hps1,*[59] and “pearl” mice (Jackson Laboratories #3215), which carry a mutation in *Hps2*, also called *Ap3b1.*[60]

Bleomycin-induced fibrosis models

Bleomycin (Hospira Inc.) was purchased from Vanderbilt University Medical Center pharmacy. Bleomycin (0.04 units) in 100 µl saline was delivered by direct i.t. instillation under anesthesia as described previously.[25,26,61] Tamoxifen-inducible transgenic mice were treated with tamoxifen (400 mg tamoxifen citrate /kg of chow ad libitum) for 2 weeks prior to bleomycin instillation (4 weeks prior to bleomycin

instillation). Lungs were harvested following euthanasia by pentobarbital at designated time points. Right lungs were tied off and snap frozen for estimation of collagen and extraction of RNA and protein, and left lungs were inflated to 25 cm H20 with 10% neutral buffered formalin for histology.

Mice were randomized to receive either 25 mg/kg/day CPI211 (ifetroban; Cumberland Pharmaceuticals, Nashville, TN) in drinking water or normal drinking water (vehicle). In a follow-up experiment, 50 mg/kg/day ozagrel HCl hydrate (CombiBlocks, San Diego, CA) was given to mice, and several mice were alternatively treated with ethanol vehicle as negative controls. Final concentration of ethanol in drinking water was approximately 0.04%. All drugs were pretested for palatability to ensure normal consumption of drinking water. Mice were weighed and water was changed once a week.

Radiation-induced fibrosis model

10-12 week-old male/female mice were randomly assigned to vehicle- or Ifetroban-treated groups. Isoflurane anesthetized mice were placed on a 37°C recirculating water heating pad and the thorax was administered 17 Gy (300 kVp/10 mA X-rays) at 1.64 Gy per min as we previously described.[62] With the exception of the thorax the entire animal was shielded by a custom lead block 2.5 cm thick.

Measurement of collagen (*in vivo*)

Total collagen in right upper lobes or whole right lungs of the lung was measured using the hydroxyproline assay (Biovision, kit #K555) or Sircol assay (Biocolor S1000 kit) as per the manufacturer's instructions and as previously published[61].

Treatment with F2-IsoPs or U46619 (*in vitro*)

Cells were seeded at a density of 8×10^4 cells/ml in DMEM supplemented with 20% FBS and allowed to grow to confluence. Twelve hours before the treatment by F2-IsoPs or U46619, the medium was changed to DMEM with 2.5% FBS and 50 µg/ml ascorbic acid. Three hours before the treatment by F2-IsoPs or U46619, Ifetroban (300nM) was added to the culture media. Cells were then treated with either 15-F2-IsoPs (100nM) (Cayman Chemical, USA) or with TBXA2R-agonist, U46619 (Cayman Chemical, USA) in the same concentration. A stock solution of 15-F2t-IsoPs and U46619 (both 1 mg/ml in ethanol) was diluted to a concentration of 10^{-5} M and then further diluted to final concentrations with DMEM.

Measurement of collagen (*in vitro*)

Cells were grown to confluence in 60–mm dishes and the medium was replaced with DMEM containing 2.5% FBS. The cells were incubated with either F2-IsoPs or TxB2 (Cayman Chemical, Ann Arbor, MI) for 48 h at 37°C. In some experiments, Ifetroban or Z-LLY-FMK (Abcam) was added 3h before stimulation, respectively. The amount of total soluble collagen in culture supernatants was measured by the Sircol dye binding assay kit (BioColor Ltd.) according to the manufacturer's protocol.

Mouse lung fibroblast culture

At the time of harvest, the lungs were perfused blood free with 30 ml PBS containing 10 U/ml heparin from the right ventricle, then minced and digested in an enzyme cocktail of DMEM containing 1% of BSA , 2 mg/ml of collagenase type IV, 100 ug/ml of DNase, and 2.5 mg of Dispase II (Roche Diagnostics, Mannheim, Germany) at 37°C for 30 min, then strained through a 100-um nylon cell strainer. Mouse lung cells were pretreated with anti-CD16/32 antibody (BioLegend) to block Fc receptors and then incubated with specific antibodies at 4°C in the dark. Lung fibroblasts were isolated by FACS Aria, defined as CD140a+/CD31-/CD45-/CD326-. Cells were isolated from 3-5 mice per group for each experiment.

Isolation and culture of primary human lung fibroblasts

Primary lung fibroblasts were isolated from IPF lungs removed at the time of lung transplant surgery as previously described[63,64].

Ex-vivo TBXA2R deletion

Cre recombinase activity was induced by 4-hydroxytamoxifen (4-OH TAM) (Sigma) at a dose of 0.2 μM, which was added into cell culture medium for 8 days. After 8 days of treatment the dose of 4-OH TAM was decreased to 0.05 μM and kept at this level until the end of experiments. Fresh 4-OH TAM was added every 2 days for MLFs. Excision of *TBXA2R* exon 2 was confirmed by PCR analysis on days 1–8 of treatment in MLFs.

Transient transfection and dual-luciferase assay of murine lung fibroblasts (MLF), human lung fibroblasts (HLF)

MLFs, and HLFs were seeded at a density of 60,000 cells/well into 24-well plates. Cells were transfected with Smad Binding Element (SBE) reporter containing a mixture of 40:1 SBE luciferase and CMV *Renilla* (Qiagen, Valencia, CA), using Lipofectamine 2000 reagent (Invitrogen, Carlsbad, CA). Transfection solutions were replaced by phenol-free medium with DMEM with 10%FBS 4 h after transfection. Forty-eight hours after transfection, cells were treated with and without several concentration of F2-IsoPs and U46619. Cells were treated for the indicated time (8h) prior to cell lysis and measurement of firefly and *Renilla* luciferase luminescence using the Dual-Luciferase Reporter Assay System (Promega, Madison, WI). Twenty microliters of extracts was used for dual-luciferase assay, with 100 μL of substrate. Activity was determined using a luminometer (BioTek Instruments, Winooski, VT) for 15 seconds for each sample. Firefly luciferase luminescence was quenched by Stop and Glo buffer (Promega) for 30 seconds before measuring *Renilla* activity. Luciferase activities of each transfection were normalized by *Renilla* activity. A value of 1.0 indicates the basal normalized activity without any added treatment, and values >1 represent the fold of induction for each reporter construct. Each experiment was performed three times to obtain means and standard errors of the mean.

Measurement of F2-IsoPs and TxB2

The levels of F2-IsoPs and TxB2 in lung tissues were determined by gas chromatography- mass spectrometry as previously described[65,66].

Immunoblotting

Western blotting was performed as previously described[67]. PVDF membranes were used for transfer, and antibodies used include anti-phospho-SMAD2/3 (1:1,000; Cell Signaling Technology, Danvers, MA), anti-phospho-Akt (1:3000; Cell Signaling Technology), anti-phospho-p44/42 (1:1000; Cell Signaling Technology), anti-Timp1 (1:3000; Thermo Fisher Scientific, Waltham, MA), anti-alpha smooth muscle Actin (1:5000; Abcam, Cambridge, UK), anti-TBXA2R (1:3000; Proteintech, Rosemont, IL), anti-HSP-70 (1:3000; Abcam), and anti-beta Actin (1:5000; Abcam). All antibodies to phosphorylated proteins were diluted in 5% BSA/TBST, and the rest were diluted in 2% milk/TBST.

Flow Cytometry of Lung Cells

Flow Cytometry of mouse lung cells were performed as previously described[68]. In brief, mouse lung cells were pretreated with anti-CD16/32 antibody (BioLegend, San Diego, CA) to block Fc receptors and then incubated with specific antibodies at 4°C in the dark. The following antibodies were used for cell surface staining: anti-CD31-FITC (BioLegend), anti-CD45-APC (BioLegend), anti-CD45-PE (BioLegend), anti-CD326-APC/Cy7 (BioLegend), anti-CD140a-PE (BioLegend), anti-CD11b-Pacific Blue (BioLegend), anti-CD103-PE (BioLegend), anti-F4/80-APC (BioLegend), anti-CD11c-PE/Cy7 (BioLegend), anti-Ly6G-APC/Cy7 (BioLegend), and 7AAD (BioLegend). To assess DNA degradation (apoptosis), the cells were incubated with 10 μg/ml of Hoechst 34580 (Life Technologies, GrandIsland, NY) for 30min at 37°C in the dark. Cell fluorescence was measured with the FACS Canto II instrument (Becton Dickinson, San Jose, CA) and analyzed by employing FlowJo software (Tree Star, San Carlos, CA). We defined MLFs as $CD31^-/CD45^-/CD326^-/CD140a^+$ lung cells, and murine lung epithelial cells as $CD31^-/CD45^-/CD326^+$ lung cells as previously reported. For immune/inflammatory cells, we defined IMs as $CD45^+/CD11b^{high}/F4/80^{high}/Ly6G^-/CD11c^+$ lung cells, AMs as $CD45^+/CD11b^{moderate}/CD11c^+/CD103^-$ lung cells, DCs as $F4/80^{high}/Ly6G^-/CD11c^+/CD103^+$ lung cells, monocytes as $CD45^+/CD11b^{high}/F4/80^{high}/Ly6G^-/CD11c^-$ lung cells, and neutrophils as $CD45^+/CD11b^{high}/Ly6G^+$ lung cells using our previously published protocol[68] (Extended Fig. 4b).

Single-cell RNA-sequencing analysis

Single-cell RNA-sequencing (scRNA-seq) data generated from single-cell suspensions generated from pulmonary fibrosis and nonfibrotic control lungs underwent quality control filtering and unbiased clustering followed by cell-type annotation as previously reported[6]. Raw and processed 10X genomics data can be found on GEO using accession number: GSE135893. The code used to analyze the data can be found at https://github.com/tgen/banovichlab/.

Statistics

Values are expressed as mean ± SEM, and sample size is given for each figure. Two-way analysis of variance (ANOVA) or 1-way ANOVA followed by the Sidak post-test was performed on Prism (GraphPad, San Diego, CA) to determine statistical significance.

Declarations

Study Approval: All studies involving human samples were approved by the Vanderbilt Institutional Review Board (IRB #'s 060165, 171657, 192004). Subjects provided informed consent prior to the collection of samples used in these studies. All animal studies were approved by the IACUC at Vanderbilt University.

Acknowledgements:

This work was supported by The National Institutes of Health (NIH) R01HL151016 (TSB), R01HL135011 (EJC), R01HL095797 (JDW), P01HL108800 (JDW), P01HL092870 (TSB), K08HL130595 (JAK), R01HL145372(JAK/NEB), R01HL119503 (LRY), K24HL143281 (LRY), Doris Duke Charitable Foundation (JAK). Ifebtroban was provided by Cumberland Pharmaceuticals.

Author Contributions

TS performed experiments, drafted the manuscript, and had intellectual input into experimental design. JC, XC, TPS, VVP, SG, WH, AR, HT all assisted with specific experiments and assays. JAK and NEB provided and analyzed scRNA-seq data. MLF assisted with radiation experiments, LRY and PG performed the HPS mouse experiments, YT, EC, JJG, JAK, TSB, and JDW conceived of the project, designed experiments, drafted and revised the manuscript.

References

1. Lederer, D. J. & Martinez, F. J. Idiopathic Pulmonary Fibrosis. *N. Engl. J. Med.* **378**, 1811–1823 (2018).
2. Hewlett, J. C., Kropski, J. A. & Blackwell, T. S. Idiopathic pulmonary fibrosis: Epithelial-mesenchymal interactions and emerging therapeutic targets. *Matrix Biol.* **71-72**, 112–127 (2018).
3. Pardo, A. & Selman, M. Idiopathic pulmonary fibrosis: new insights in its pathogenesis. *Int. J. Biochem. Cell Biol.* **34**, 1534–1538 (2002).
4. Winters, N. I., Burman, A., Kropski, J. A. & Blackwell, T. S. Epithelial Injury and Dysfunction in the Pathogenesis of Idiopathic PulmonaryFibrosis. *Am. J. Med. Sci.* **357**, 374–378 (2019).
5. Adams, T. S. *et al.* Single Cell RNA-seq reveals ectopic and aberrant lung resident cell populations in Idiopathic Pulmonary Fibrosis. *bioRxiv* 759902 (2019) doi:10.1101/759902.
6. Habermann, A. C. *et al.* Single-cell RNA-sequencing reveals profibrotic roles of distinct epithelial and mesenchymal lineages in pulmonary fibrosis. *bioRxiv* 753806 (2019) doi:10.1101/753806.

7. King, T. E., Jr *et al.* A phase 3 trial of pirfenidone in patients with idiopathic pulmonary fibrosis. *N. Engl. J. Med.* **370**, 2083–2092 (2014).
8. Richeldi, L. *et al.* Efficacy and safety of nintedanib in idiopathic pulmonary fibrosis. *N. Engl. J. Med.* **370**, 2071–2082 (2014).
9. Iyer, S. S. *et al.* Oxidation of extracellular cysteine/cystine redox state in bleomycin-induced lung fibrosis. *Am. J. Physiol. Lung Cell. Mol. Physiol.* **296**, L37–45 (2009).
10. Cheresh, P., Kim, S.-J., Tulasiram, S. & Kamp, D. W. Oxidative stress and pulmonary fibrosis. *Biochim. Biophys. Acta* **1832**, 1028–1040 (2013).
11. Hecker, L. *et al.* NADPH oxidase-4 mediates myofibroblast activation and fibrogenic responses to lung injury. *Nat. Med.* **15**, 1077–1081 (2009).
12. Mont, S. *et al.* Accumulation of isolevuglandin-modified protein in normal and fibrotic lung. *Sci. Rep.* **6**, 24919 (2016).
13. Montuschi, P., Barnes, P. J. & Roberts, L. J., 2nd. Isoprostanes: markers and mediators of oxidative stress. *FASEB J.* **18**, 1791–1800 (2004).
14. Comporti, M. *et al.* F2-isoprostanes are not just markers of oxidative stress. *Free Radic. Biol. Med.* **44**, 247–256 (2008).
15. Comporti, M. *et al.* F2-isoprostanes stimulate collagen synthesis in activated hepatic stellate cells: a link with liver fibrosis? *Lab. Invest.* **85**, 1381–1391 (2005).
16. Gardi, C. *et al.* F2-isoprostane receptors on hepatic stellate cells. *Lab. Invest.* **88**, 124–131 (2008).
17. Cyphert, J. M. *et al.* Allergic inflammation induces a persistent mechanistic switch in thromboxane-mediated airway constriction in the mouse. *Am. J. Physiol. Lung Cell. Mol. Physiol.* **302**, L140–51 (2012).
18. Dogné, J.-M., de Leval, X., Benoit, P., Delarge, J. & Masereel, B. Thromboxane A2 inhibition: therapeutic potential in bronchial asthma. *Am. J. Respir. Med.* **1**, 11–17 (2002).
19. Montuschi, P. *et al.* 8-Isoprostane as a biomarker of oxidative stress in interstitial lung diseases. *Am. J. Respir. Crit. Care Med.* **158**, 1524–1527 (1998).
20. Schmitt, D. *et al.* Leukocytes utilize myeloperoxidase-generated nitrating intermediates as physiological catalysts for the generation of biologically active oxidized lipids and sterols in serum. *Biochemistry* **38**, 16904–16915 (1999).
21. Ma, W. *et al.* Calpain mediates pulmonary vascular remodeling in rodent models of pulmonary hypertension, and its inhibition attenuates pathologic features of disease. *J. Clin. Invest.* **121**, 4548–4566 (2011).
22. Quiniou, C. *et al.* Dominant role for calpain in thromboxane-induced neuromicrovascular endothelial cytotoxicity. *J. Pharmacol. Exp. Ther.* **316**, 618–627 (2006).
23. Ogletree, M. L., Harris, D. N., Schumacher, W. A., Webb, M. L. & Misra, R. N. Pharmacological profile of BMS 180,291: a potent, long-acting, orally active thromboxane A2/prostaglandin endoperoxide receptor antagonist. *J. Pharmacol. Exp. Ther.* **264**, 570–578 (1993).

24. Degryse, A. L. *et al.* TGFβ signaling in lung epithelium regulates bleomycin-induced alveolar injury and fibroblast recruitment. *Am. J. Physiol. Lung Cell. Mol. Physiol.* **300**, L887–97 (2011).
25. Lawson, W. E. *et al.* Endoplasmic reticulum stress enhances fibrotic remodeling in the lungs. *Proc. Natl. Acad. Sci. U. S. A.* **108**, 10562–10567 (2011).
26. Tanjore, H. *et al.* Alveolar epithelial cells undergo epithelial-to-mesenchymal transition in response to endoplasmic reticulum stress. *J. Biol. Chem.* **286**, 30972–30980 (2011).
27. Sisson, T. H. *et al.* Targeted injury of type II alveolar epithelial cells induces pulmonary fibrosis. *Am. J. Respir. Crit. Care Med.* **181**, 254–263 (2010).
28. Vicary, G. W., Vergne, Y., Santiago-Cornier, A., Young, L. R. & Roman, J. Pulmonary Fibrosis in Hermansky-Pudlak Syndrome. *Ann. Am. Thorac. Soc.* **13**, 1839–1846 (2016).
29. Young, L. R. *et al.* The alveolar epithelium determines susceptibility to lung fibrosis in Hermansky-Pudlak syndrome. *Am. J. Respir. Crit. Care Med.* **186**, 1014–1024 (2012).
30. Young, L. R. *et al.* Epithelial-macrophage interactions determine pulmonary fibrosis susceptibility in Hermansky-Pudlak syndrome. *JCI Insight* **1**, e88947 (2016).
31. Young, L. R., Pasula, R., Gulleman, P. M., Deutsch, G. H. & McCormack, F. X. Susceptibility of Hermansky-Pudlak mice to bleomycin-induced type II cell apoptosis and fibrosis. *Am. J. Respir. Cell Mol. Biol.* **37**, 67–74 (2007).
32. Anathy, V. *et al.* Reducing protein oxidation reverses lung fibrosis. *Nat. Med.* **24**, 1128–1135 (2018).
33. Bocchino, M. *et al.* Reactive oxygen species are required for maintenance and differentiation of primary lung fibroblasts in idiopathic pulmonary fibrosis. *PLoS One* **5**, e14003 (2010).
34. Sambo, P. *et al.* Oxidative stress in scleroderma: maintenance of scleroderma fibroblast phenotype by the constitutive up-regulation of reactive oxygen species generation through the NADPH oxidase complex pathway. *Arthritis Rheum.* **44**, 2653–2664 (2001).
35. Hecker, L. *et al.* Reversal of persistent fibrosis in aging by targeting Nox4-Nrf2 redox imbalance. *Sci. Transl. Med.* **6**, 231ra47 (2014).
36. Sanders, Y. Y. *et al.* Histone deacetylase inhibition promotes fibroblast apoptosis and ameliorates pulmonary fibrosis in mice. *Eur. Respir. J.* **43**, 1448–1458 (2014).
37. Sanders, Y. Y. *et al.* Histone modifications in senescence-associated resistance to apoptosis by oxidative stress. *Redox Biol* **1**, 8–16 (2013).
38. Bauer, J. *et al.* Pathophysiology of isoprostanes in the cardiovascular system: implications of isoprostane-mediated thromboxane A2 receptor activation. *Br. J. Pharmacol.* **171**, 3115–3131 (2014).
39. Acquaviva, A., Vecchio, D., Arezzini, B., Comporti, M. & Gardi, C. Signaling pathways involved in isoprostane-mediated fibrogenic effects in rat hepatic stellate cells. *Free Radic. Biol. Med.* **65**, 201–207 (2013).
40. Fois, A. G. *et al.* Evaluation of oxidative stress biomarkers in idiopathic pulmonary fibrosis and therapeutic applications: a systematic review. *Respir. Res.* **19**, 51 (2018).

41. Psathakis, K. *et al.* Exhaled markers of oxidative stress in idiopathic pulmonary fibrosis. *Eur. J. Clin. Invest.* **36**, 362–367 (2006).
42. Malli, F. *et al.* 8-isoprostane levels in serum and bronchoalveolar lavage in idiopathic pulmonary fibrosis and sarcoidosis. *Food Chem. Toxicol.* **61**, 160–163 (2013).
43. Arezzini, B., Vecchio, D., Signorini, C., Stringa, B. & Gardi, C. F2-isoprostanes can mediate bleomycin-induced lung fibrosis. *Free Radic. Biol. Med.* **115**, 1–9 (2018).
44. Marinković, A., Liu, F. & Tschumperlin, D. J. Matrices of physiologic stiffness potently inactivate idiopathic pulmonary fibrosis fibroblasts. *Am. J. Respir. Cell Mol. Biol.* **48**, 422–430 (2013).
45. Hinz, B. & Lagares, D. Evasion of apoptosis by myofibroblasts: a hallmark of fibrotic diseases. *Nat. Rev. Rheumatol.* **16**, 11–31 (2020).
46. Liu, F. *et al.* Mechanosignaling through YAP and TAZ drives fibroblast activation and fibrosis. *Am. J. Physiol. Lung Cell. Mol. Physiol.* **308**, L344–57 (2015).
47. Haak, A. J. *et al.* Selective YAP/TAZ inhibition in fibroblasts via dopamine receptor D1 agonism reverses fibrosis. *Sci. Transl. Med.* **11**, (2019).
48. Jain, M. *et al.* Mitochondrial reactive oxygen species regulate transforming growth factor-β signaling. *J. Biol. Chem.* **288**, 770–777 (2013).
49. Koli, K., Myllärniemi, M., Keski-Oja, J. & Kinnula, V. L. Transforming growth factor-beta activation in the lung: focus on fibrosis and reactive oxygen species. *Antioxid. Redox Signal.* **10**, 333–342 (2008).
50. Lodyga, M. & Hinz, B. TGF-β1 - A truly transforming growth factor in fibrosis and immunity. *Semin. Cell Dev. Biol.* (2019) doi:10.1016/j.semcdb.2019.12.010.
51. Meng, X.-M., Nikolic-Paterson, D. J. & Lan, H. Y. TGF-β: the master regulator of fibrosis. *Nat. Rev. Nephrol.* **12**, 325–338 (2016).
52. Bots, M. L. *et al.* Thromboxane prostaglandin receptor antagonist and carotid atherosclerosis progression in patients with cerebrovascular disease of ischemic origin: a randomized controlled trial. *Stroke* **45**, 2348–2353 (2014).
53. Dogné, J.-M. *et al.* Therapeutic potential of thromboxane inhibitors in asthma. *Expert Opin. Investig. Drugs* **11**, 275–281 (2002).
54. Gaussem, P. *et al.* The specific thromboxane receptor antagonist S18886: pharmacokinetic and pharmacodynamic studies. *J. Thromb. Haemost.* **3**, 1437–1445 (2005).
55. Malini, P. L., Strocchi, E., Zanardi, M., Milani, M. & Ambrosioni, E. Thromboxane antagonism and cough induced by angiotensin-converting-enzyme inhibitor. *Lancet* **350**, 15–18 (1997).
56. Guth, B. D. *et al.* Pharmacokinetics and pharmacodynamics of terbogrel, a combined thromboxane A2 receptor and synthase inhibitor, in healthy subjects. *Br. J. Clin. Pharmacol.* **58**, 40–51 (2004).
57. Hussein, Z. *et al.* Characterization of the pharmacokinetics and pharmacodynamics of a new oral thromboxane A2-receptor antagonist AA-2414 in normal subjects: population analysis. *Clin. Pharmacol. Ther.* **55**, 441–450 (1994).

58. Badea, T. C., Wang, Y. & Nathans, J. A noninvasive genetic/pharmacologic strategy for visualizing cell morphology and clonal relationships in the mouse. *J. Neurosci.* **23**, 2314–2322 (2003).
59. Lyerla, T. A. *et al.* Aberrant lung structure, composition, and function in a murine model of Hermansky-Pudlak syndrome. *Am. J. Physiol. Lung Cell. Mol. Physiol.* **285**, L643–53 (2003).
60. Feng, L., Rigatti, B. W., Novak, E. K., Gorin, M. B. & Swank, R. T. Genomic structure of the mouse Ap3b1 gene in normal and pearl mice. *Genomics* **69**, 370–379 (2000).
61. Burman, A. *et al.* Localized hypoxia links ER stress to lung fibrosis through induction of C/EBP homologous protein. *JCI Insight* **3**, (2018).
62. Traver, G. *et al.* Loss of Nrf2 promotes alveolar type 2 cell loss in irradiated, fibrotic lung. *Free Radic. Biol. Med.* **112**, 578–586 (2017).
63. West, J. D. *et al.* Identification of a common Wnt-associated genetic signature across multiple cell types in pulmonary arterial hypertension. *Am. J. Physiol. Cell Physiol.* **307**, C415–30 (2014).
64. Hemnes, A. R. *et al.* Critical Genomic Networks and Vasoreactive Variants in Idiopathic Pulmonary Arterial Hypertension. *Am. J. Respir. Crit. Care Med.* **194**, 464–475 (2016).
65. Kirkby, N. S. *et al.* Cyclooxygenase-1, not cyclooxygenase-2, is responsible for physiological production of prostacyclin in the cardiovascular system. *Proc. Natl. Acad. Sci. U. S. A.* **109**, 17597–17602 (2012).
66. Milne, G. L., Sanchez, S. C., Musiek, E. S. & Morrow, J. D. Quantification of F2-isoprostanes as a biomarker of oxidative stress. *Nat. Protoc.* **2**, 221–226 (2007).
67. West, J. D. *et al.* Antagonism of the thromboxane-prostanoid receptor is cardioprotective against right ventricular pressure overload. *Pulm. Circ.* **6**, 211–223 (2016).
68. Zaynagetdinov, R. *et al.* Identification of myeloid cell subsets in murine lungs using flow cytometry. *Am. J. Respir. Cell Mol. Biol.* **49**, 180–189 (2013).

Figures

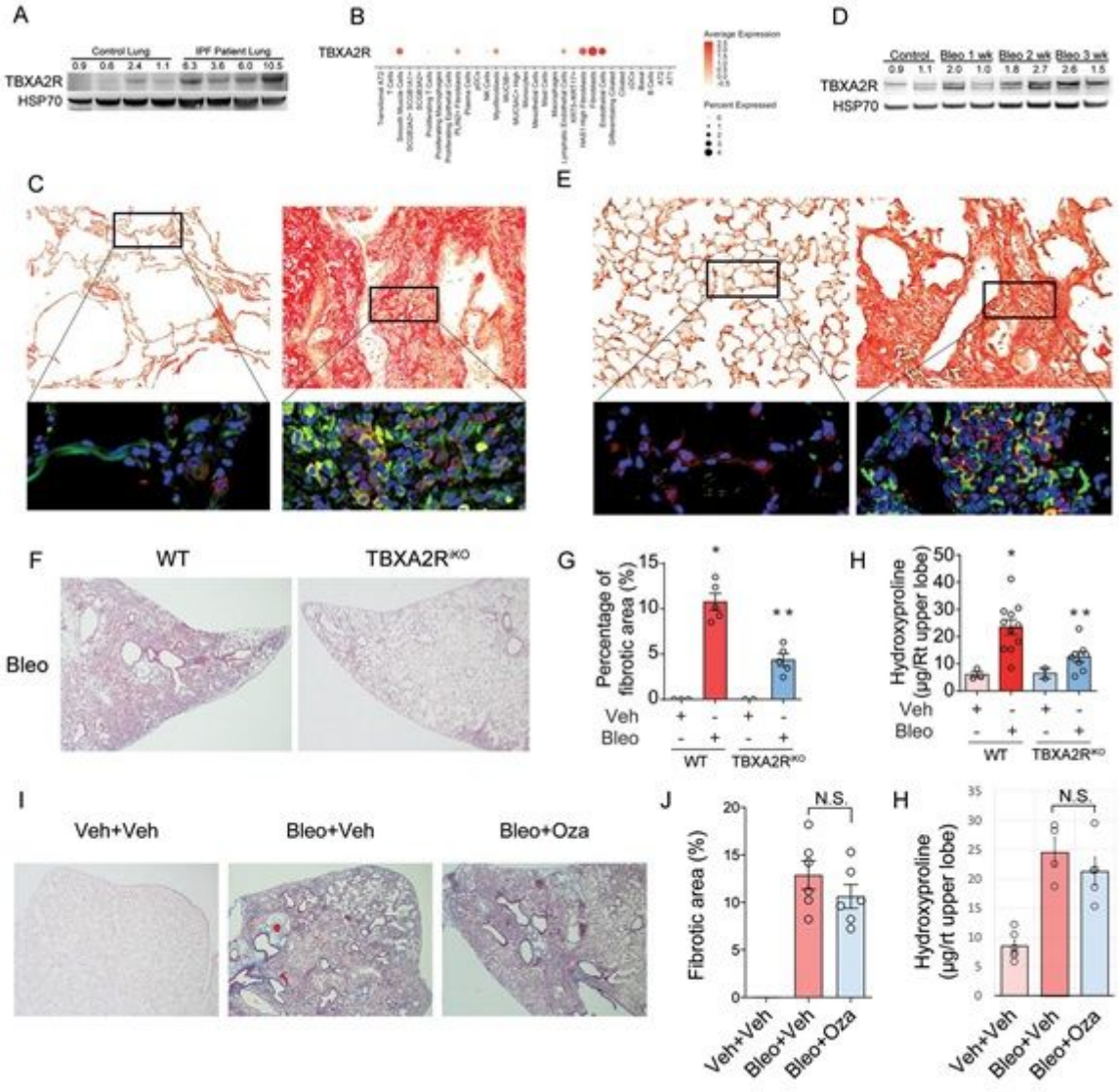

Figure 1

TBXA2R is upregulated in fibroblasts during lung fibrosis and deleting TBXA2R protects against experimental lung fibrosis A) Western blot for TBXA2R in lung tissue from IPF patients compared to non-diseased controls. B) Dotplot depicting TBXA2R gene expression in jointly analyzed scRNA-seq data from explanted lungs of 20 pulmonary fibrosis patients and 10 non-diseased controls (primary data from reference 6). C) Representative immunostaining for TBXA2R in IPF and control lung sections. TBXA2R is red, and S100A4 is green. D) Western blot for TBXA2R expression in lungs of mice at baseline and 1-3 weeks after intratracheal bleomycin. E) Immunostaining for TBXA2R in mouse lung sections at 3 weeks after treatment with vehicle (control) or bleomycin. TBXA2R is red, S100A4 is green. F) Representative Masson's trichrome-stained lung sections from wild-type (WT) and TBXA2RiKO mice at 21 days after intratracheal bleomycin (bleo). G) Morphometric evaluation of lung fibrosis on lung sections. N = 3 for control WT and TBXA2RiKO mice, and N=5 for the Bleo treatment groups. *p<0.05 compared to all other groups, **p<0.05 compared to bleomycin-treated WT group (by ANOVA with Tukey's HSD). H)

Hydroxyproline content in the right upper lobe. N=3 for control WT mice, N=2 for control TBXA2RiKO mice, N=11 for the Bleo-treated WT mice, and N=8 for the Bleo-treated TBXA2RiKO mice. *p<0.05 compared to all other groups, **p<0.05 compared to bleomycin-treated WT group (by ANOVA with Tukey's HSD). I) Representative Masson's trichrome-stained lung sections from WT mice at 21 days after treatment with intratracheal bleomycin (bleo) or vehicle (veh), with or without thromboxane synthesis inhibitor (Ozagrel, Oza) beginning on day 7. J) Morphometric evaluation of lung fibrosis on lung sections. N=5 for each group. N.S.; not significant. K) Hydroxyproline content in right upper lobe. N=6 for each group. *p<0.05 compared to all other groups, **p<0.05 compared to bleomycin-treated WT group.

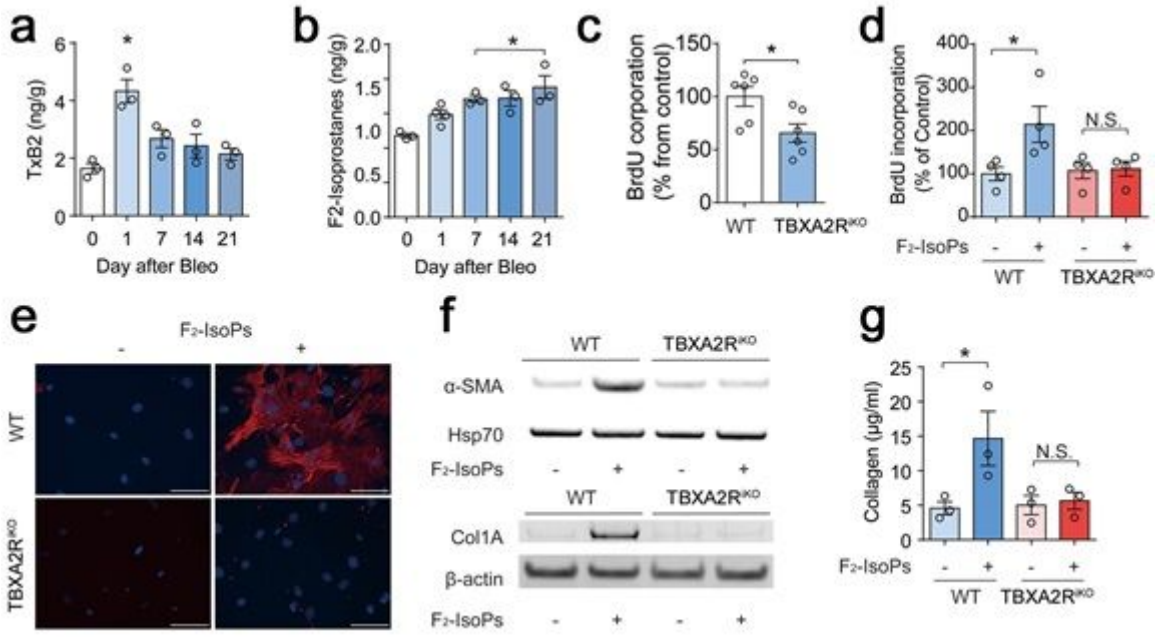

Figure 2

F2-isoprostanes activate TBXA2R signaling in fibrosis. A) Thromboxane B2 (TxB2) was measured in the lungs of mice at baseline and 1-3 weeks after bleo. N=3 per group, *p<0.05 compared to baseline. B) F2-Isoprostanes measured in the lungs of mice at baseline and 1-3 weeks after intratracheal bleomycin (bleo). N=3-4 per group, *p<0.05 compared to baseline. C) Primary lung fibroblasts from Rosa-creER/Tbxa2rf/f mice were treated ex-vivo with 4OH-tamoxifen to obtain TBXA2R-deleted fibroblasts (TBXA2RiKO) and BrdU incorporation was measured at 48 hours under full serum (10%) conditions. N=6 mice per group, *p<0.05 compared to WT fibroblasts. D) F2-Isoprostanes (F2-IsoPs, 100 nM) stimulation of WT and Tbxa2riKO fibroblasts under reduced serum conditions (2.5%) measured at 48 hours. N = 4 per group, *p<0.05. E) Immunocytochemistry evaluating for α-SMA expression 48 hours after F2-IsoPs treatment. α-SMA; red, DAPI; blue. (F-G) Western blot for I) α-SMA and F) collagen 1expression at 48 hours after F2-IsoP treatment. G) Densitometry for collagen 1. N=3 lungs/condition.

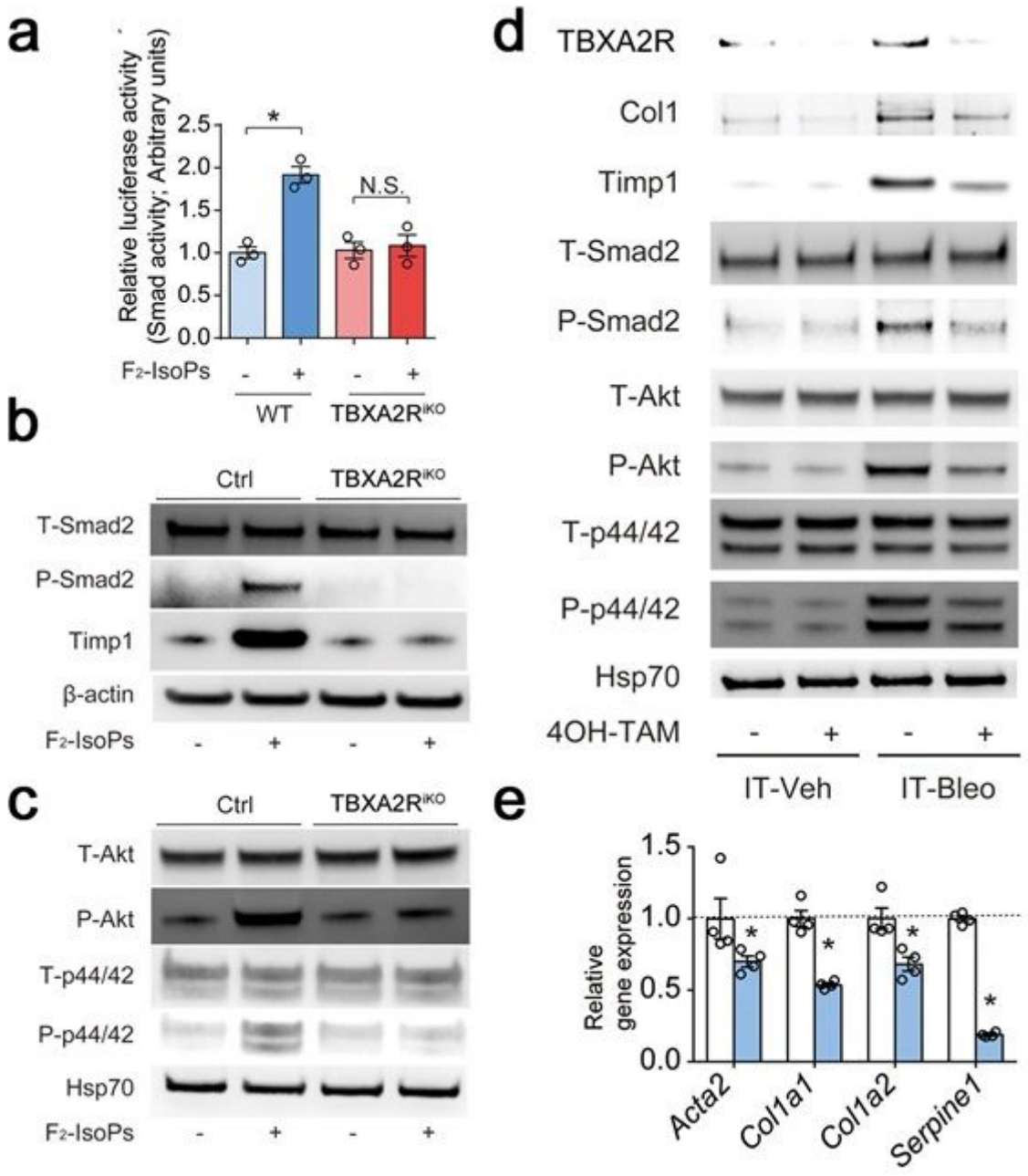

Figure 3

F2-isoprostane induction of the TGFβ pathway requires TBXA2R. A) Luciferase assay was performed to quantify Smad2/3 transcriptional activity after transfection with SBE-driven luciferase reporter construct using WT and Tbxa2riKO lung fibroblasts at 8 hours after F2-IsoP or vehicle treatment. N=3 for each group, *p<0.05. B) Western blot for total Smad2 (T-Smad2), phospho-Smad2 (P-Smad2) and Timp1 using WT and Tbxa2riKO lung fibroblasts at 24 hours after F2-IsoP or vehicle treatment. C) Western blot for total Akt (T-Akt), phospho-Akt (P-Akt), total-p44/42 (T-p44/42) and phospho-p44/42 (P-p44/42) using WT and Tbxa2riKO lung fibroblasts at 24 hours after F2-IsoP or vehicle treatment. Western blots were performed in triplicate samples and repeated at least twice. Significance determined by ANOVA with Tukey's HSD (parts b-e), unpaired t-test (f), multiple ANOVA with Tukey's HSD (g,k,l) D) Western blot for canonical and non-canonical TFG-β pathway markers in murine lung fibroblasts with TBXA2R knocked

out by 4OH-Tam ex-vivo. (E) Expression of TGF-β target genes compared to controls (white columns) following TBXA2R deletion (blue columns). Gene expression was normalized to HPRT, and then to expression levels in controls. *p<0.05 compared to non-induced by unpaired t-test.

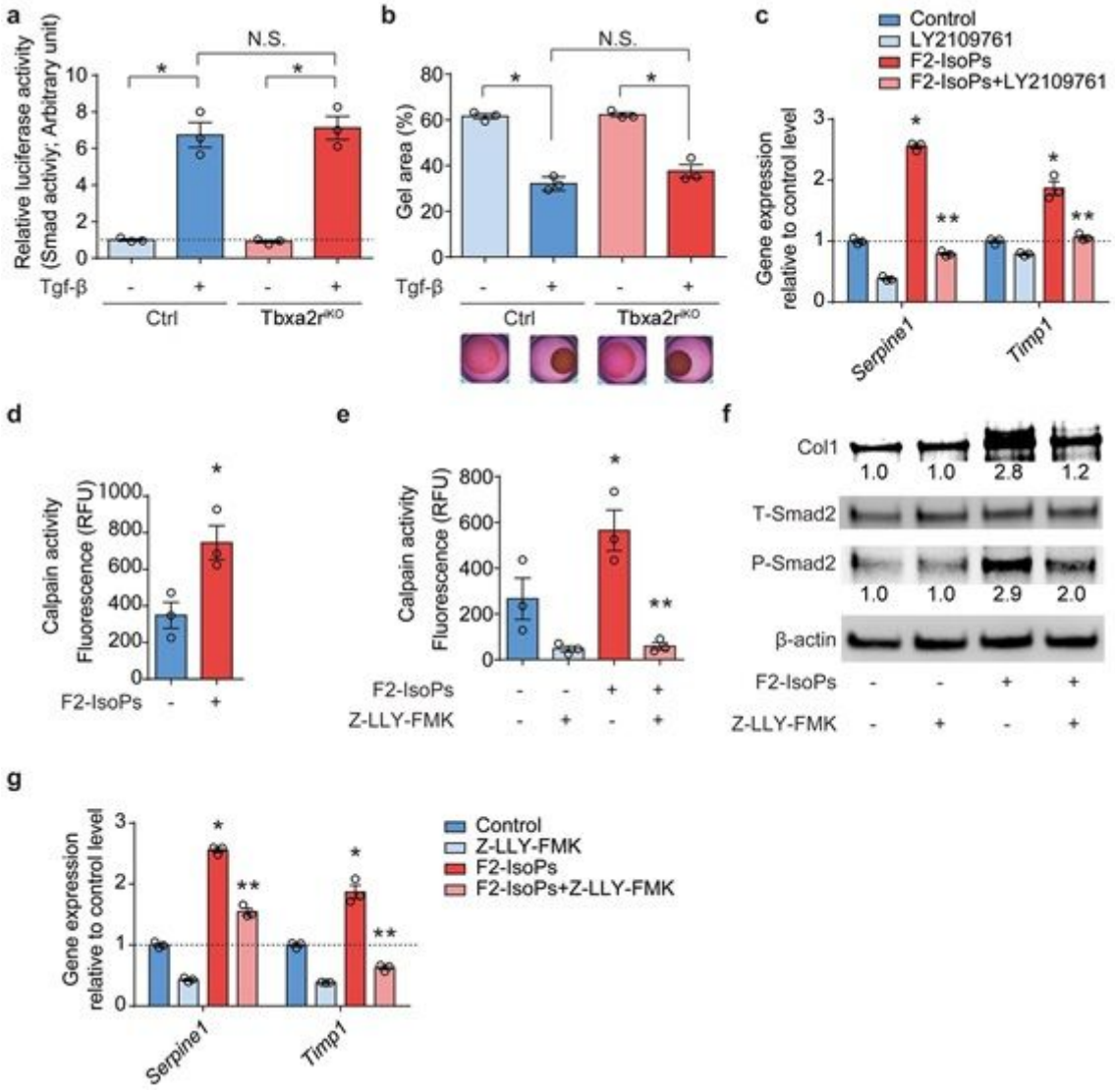

Figure 4

TBXA2R-induced calpain activity mediates TGF-β activation. A) Luciferase assay was performed to quantify Smad2/3 transcriptional activity after transfection with SBE-driven luciferase reporter construct using WT and TBXA2RiKO lung fibroblasts with or without TGF-β treatment (10 ng/ml) at 4 hours. N=3 for each group. B) WT and TBXA2RiKO fibroblasts were cultured within 3D-collagen lattices in the presence and absence of Ifetroban (300 nM) for 1 hour. After polymerization, the gels were mechanically detached from the wells and cultured in the presence and absence of TGF-β for 6 hours. Then, the contraction of the gel was quantified. N=3 for each group. *p<0.05. N.S.; not significant. C) WT mouse lung fibroblasts were treated with or without F2-Isoprostanes (F2-IsoPs, 100 nM) and LY2109761, inhibitor of TGF-β receptor type 1/type II kinases, for 24 hours. Quantitative PCR analysis for Serpine1 and Timp1 gene expression. N=3 for each group, *p<0.05 compared to control group, **p<0.05 compared to the F2-IsoPs-treated group. N.S.; not significant. D) Primary lung fibroblasts from WT mice were treated

with or without F2-IsoPs (300 nM) for 24 hours. Calpain activity was measured using a fluorescent assay. N=3 for each group, *p<0.05. (E-G) Primary lung fibroblasts from WT mice were treated with or without F2-IsoPs and calpain inhibitor (Z-LLY-FMK, 30 μM) for 24 hours. E) Calpain activity was measured using a fluorescent assay. F) Western blot for collagen 1, total-Smad2 (t-Smad2) and phospho-Smad2 (p-Smad2). Numbers indicate Collagen 1 densitometry normalized to actin and p-Smad2/t-Smad2 ratio. G) Quantitative PCR was performed for Serpine1, Col1a1, Col1a2 and Acta2. N=3 for each group, *p<0.05 compared to all other groups. Significance was determined by two-way ANOVA with Tukey's HSD (all quantitative figure elements).

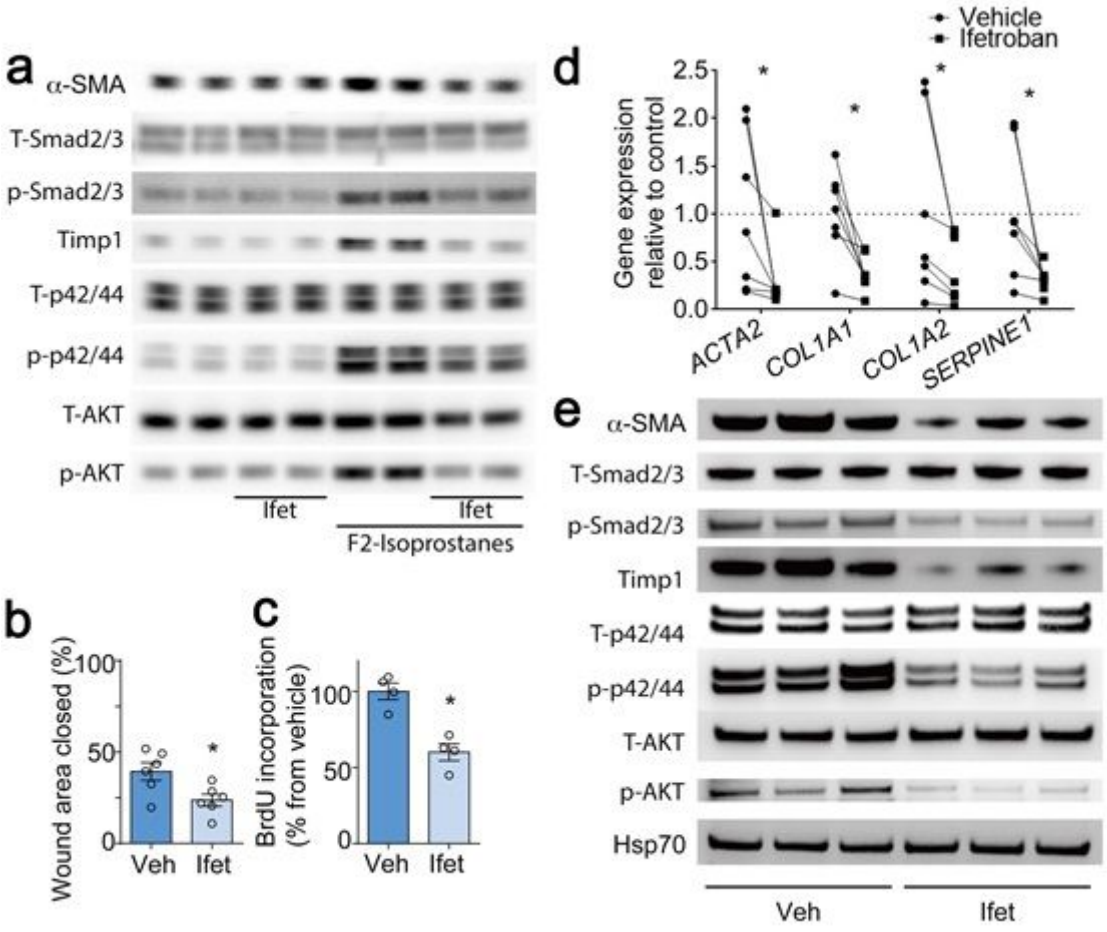

Figure 5

TBXA2R antagonism reduces proliferation, migration, and activation of fibroblasts from lungs of mice and IPF patients. (A) Lung fibroblasts were isolated from lungs of mice and treated with F2-isoprostanes, ifetroban, or both. Western blot for evaluation of a-Sma, total-Smad2/3 (T-Smad2/3), phospho-Smad2/3 (P-Smad2/3), Timp1, total-p44/42 (T-p44/42), phospho-p44/42 (P-p44/42), total-Akt (T-Akt), and phospho-Akt (P-Akt). (B-E)Lung fibroblasts were isolated from explanted lungs of 6 IPF patients and treated with Ifetroban (Ifet) (300 nM) or vehicle. B) Scratch wound closure assay measured as wound area closed at 24 hours by unpaired t-test. C) Cell proliferation measured by BrdU incorporation. D) Quantitative PCR for evaluation of profibrotic gene expression. N=6 per group, *p<0.05 compared to vehicle-treated group by paired t-test E) Western blot for evaluation of total-SMAD2/3 (T-SMAD2/3),

phospho-SMAD2/3 (P-SMAD2/3), TIMP1, total-p44/42 (T-p44/42), phospho-p44/42 (P-p44/42), total-AKT (T-AKT), and phospho-AKT (P-AKT).

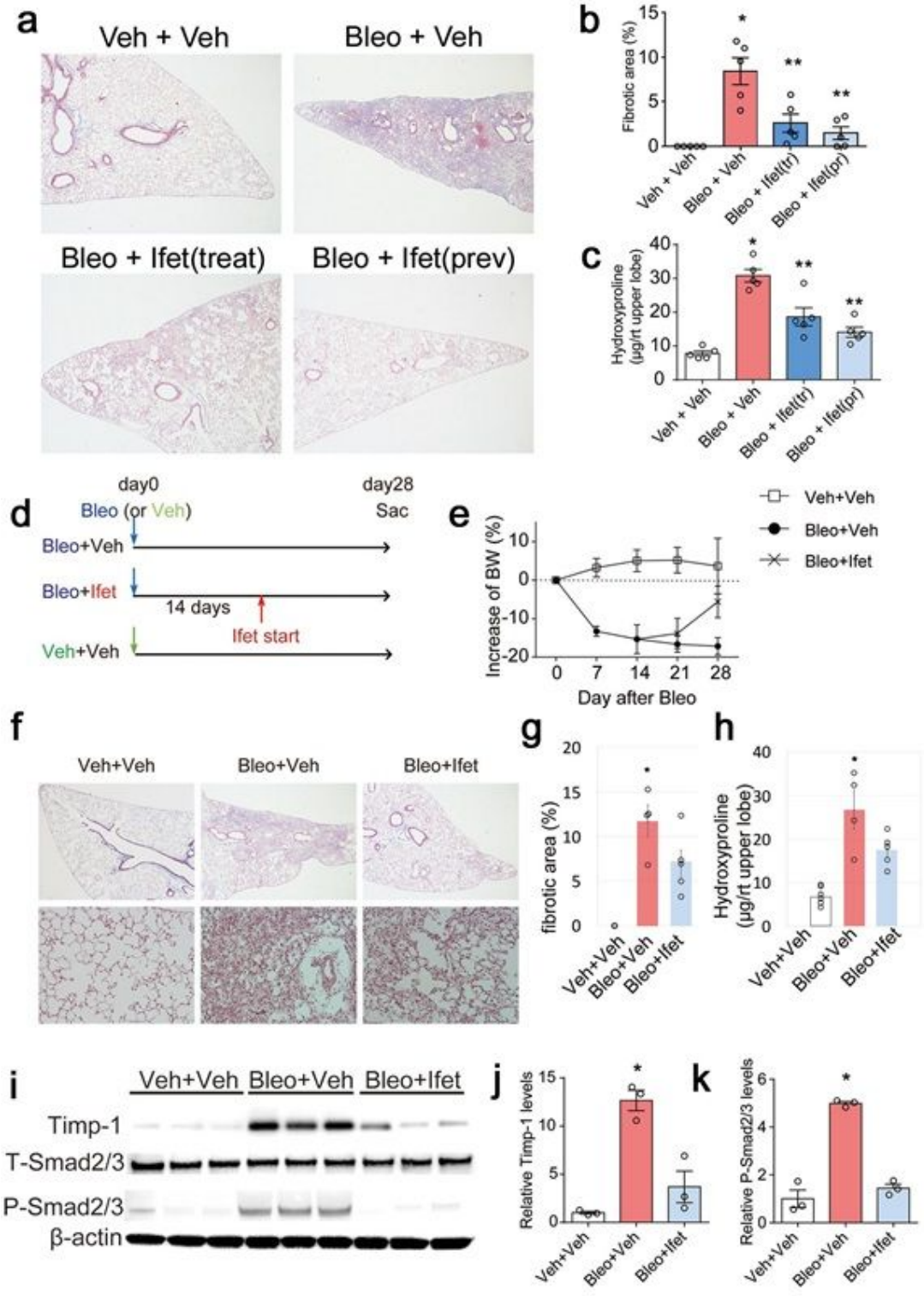

Figure 6

TBXA2R signaling regulates bleomycin-induced fibrosis, even when started 7 and 14 days after injury. (A-C, I-K) Wild-type mice were treated with intratracheal bleomycin, (bleo. 0.04 U) or vehicle, with or without Ifetroban (25 mg/kg/day). Ifetroban treatment [Ifet(treat)] was delivered from day 7 to day 21 after

bleomycin. Ifetroban prevention [Ifet(prev)] was started 3 days before bleomycin treatment and continued to day 21. A) Representative Masson's trichrome-stained lung sections. B) Morphometric evaluation of lung fibrosis using these lung sections. C) Hydroxyproline content in right upper lobe. *p<0.05 compared to Veh+Veh group, **p<0.05 compared to Bleo+Veh group (D) Experimental schema showing timing of Ifetroban start and date of sacrifice for parts E-H. (E) Change in weight following bleomycin treatment. Data are presented as means ± SEM. Significance was determined by ANOVA with repeated measures. (F) Representative Masson's trichrome-stained lung sections from wild-type mice at 28 days after treatment with intratracheal bleomycin (bleo) or vehicle (veh) with or without Ifetroban-treatment begun at day 14. (G), Morphometric evaluation of lung fibrosis on lung sections. Data are presented as means ± SEM. (H) Hydroxyproline content quantified from the right upper lobe. Data are presented as means ± SEM. *p<0.05 compared to Veh+Veh group or Bleo+Ifet group. Significance in parts D and E by ANOVA with Tukey's HSD. I) Western blot for Timp1, phospho-Smad2/3 and total-Smad2/3 in lung tissue. J) Densitometry for Timp1. *p<0.05 compared to all other groups. K) Densitometry for total and phospho-Smad2/3. (N = 5 per group). *p<0.05 compared to all other groups.

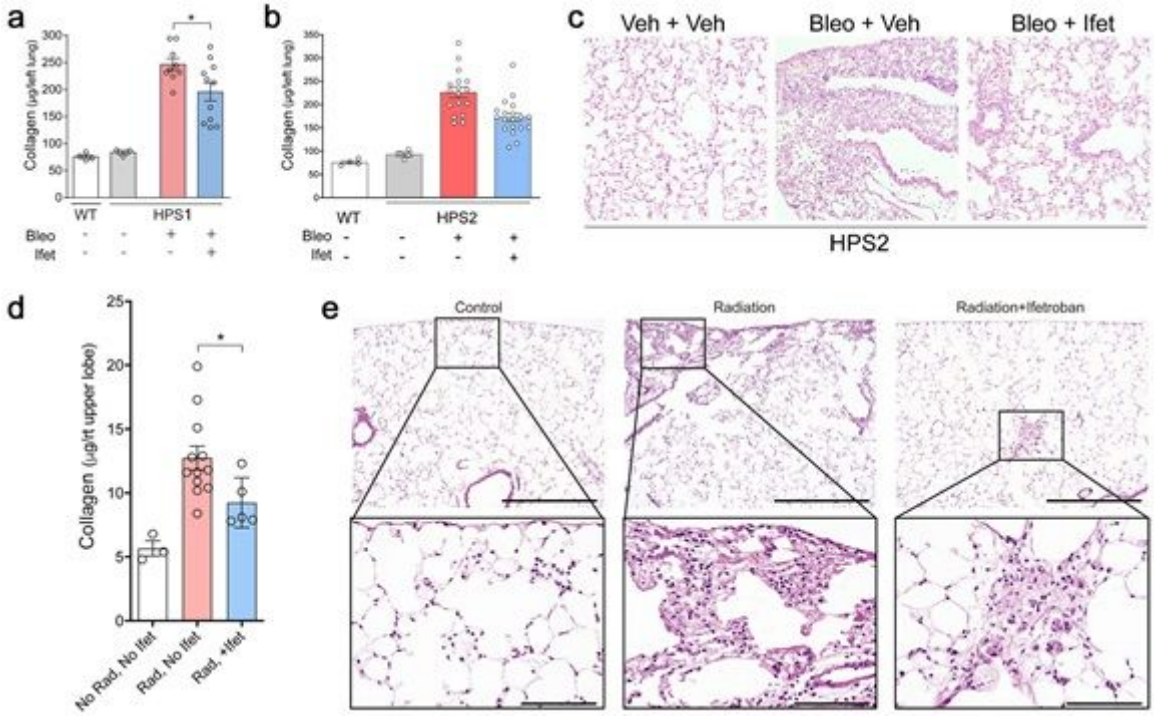

Figure 7

TBXA2R antagonism attenuates Hermansky-Pudlak syndrome (HPS)-associated fibrosis and radiation-induced fibrosis. A-B) HPS1, HPS2, or wild-type (WT) control mice were treated with Ifetroban (Ifet) or vehicle, followed by intratracheal bleomycin (0.025 U) and lungs were harvested on day 7. Sircol assay quantifying collagen content in lungs of HPS1 mice or HPS2 mice. N = 3-4 per group unchallenged mice, 9-17 per group HPS mice. C) Representative histology for HPS2 mice with or without ifetroban pretreatment. D) Sircol assay quantifying collagen content and E) representative histology from lungs of mice exposed to thoracic irradiation (17 Gy) along with Ifetroban (N = 5) or vehicle (N = 12) and harvested at 4 months post-irradiation. * p < 0.05. For all quantitative figure elements, data are presented as means

± SEM, with data from each individual mouse overlaid as circles. Statistics were performed by ANOVA, followed by Tukey's HSD for comparisons between individual groups (with * = $p<0.05$).

Supplementary Files

This is a list of supplementary files associated with this preprint. Click to download.

- EXTENDEDDATAFIGURES.pdf